Document Info: Conference Proceedings of Wireless 2000
Calgary, Alberta, Canada, July 10–12, 2000, vol. 2, pp. 627–639

Performance Investigation for Multiuser Linear and Decision-Feedback Equalizers

Ramon Schlagenhaufer*, Abu B. Sesay*, Brent R. Petersen**

* TR*Labs* / University of Calgary
280 Discovery Place One
3553 - 31 Str. N.W., Calgary, Alberta
CANADA T2L 2K7
e-mail: {schlagen,sesay}@cal.trlabs.ca

** Dept. of Electrical and Computer Engineering
University of New Brunswick
P.O. Box 4400 / Fredericton, New Brunswick
CANADA E3B 5A3
e-mail: b.petersen@ieee.org

Abstract— **This paper quantifies the effect of diversity and number of users on the performance of a wireless multiuser system. The reverse link is considered for a system with N users and a single base station. The base station receives the signal at A different antennas. In addition to antenna diversity, frequency diversity is used by transmitting signals with larger than Nyquist bandwidth. The receiver consists of a multiple-input multiple-output (MIMO) MMSE linear (LE) or decision-feedback equalizer (DFE). The quasi-stationary, frequency selective radio channels between all users and the base station are assumed to be known at the receiver. We unify the concepts of frequency and antenna diversity and show that the total degree of diversity is equal to the product of processing gain and receiver inputs. It is proven that the general relationship between the equalizer output SNR and MMSE for the MIMO LE and DFE is the same as for the single-input single-output equalizers. Bit error rates, outage probabilities and capacities of systems with different degrees of diversity, user populations and signal to noise ratios are calculated and illustrated.**

Keywords— **Multiuser detection, MIMO equalization, spread spectrum, antenna diversity, diversity combining, decision-feedback equalizers, wireless communication.**

I. Introduction

THE connection of several individual stations to a central unit is a characteristic of many modern communication systems. In the face of bandwidth limited radio channels, the rise of multimedia applications requires, in addition, highly spectrally efficient systems and very fast data rates, which causes the radio channel to behave frequency selectively. While the latter introduces intersymbol interference (ISI) in the received signals, multiple, simultaneously transmitting stations cause cochannel interference (CCI). The combined interference is known to be the major limiting factor of both system performance and capacity. Several access schemes – among them TDMA, FDMA and CDMA – can be employed to avoid or mitigate CCI. These schemes are based on bandwidth expansion. More recently, it has been shown that multiple receiver inputs (antenna/spatial diversity, SDMA) have a similar ability to suppress CCI [1], [2].

This paper investigates the reverse link of a spectrally efficient, high data rate multiuser system that combines the concepts of both frequency and antenna diversity in order to increase the capacity and enable the system to support several users simultaneously. Frequency diversity is introduced by spreading the bandwidth of all system users to K-times the Nyquist bandwidth. The multiple access scheme associated with this method is spread-spectrum multiple access (SSMA). Receiving the signals at A sufficiently spaced antennas provides antenna diversity.

Several different receiver types have been developed in the past in order to separate the interfering signals and to allow for a reliable detection of all users. Among them are the conventional matched filter receiver, maximum likelihood (MLSE) detector [3], multistage detectors [4], successive and parallel interference cancellers [5], [6], and equalizer/combiner structures [7], [8]. Considering the amount of publications, the latter have proven to be highly attractive as they constitute an excellent compromise between low complexity, low performance

detectors (conventional matched filter receiver) and high complexity, high performance receivers (MLSE detector). In addition, these receivers may offer a very high spectral efficiency, which is shown subsequently. We concentrate thus on multiple-input multiple-output (MIMO) minimum mean-square error (MMSE) linear equalizers (LE) and decision-feedback equalizers (DFE) for the detection of asynchronously received signals over frequency selective, quasi-stationary radio channels.

It has been shown analytically for the MIMO zero-forcing (ZF) LE that the maximal number of supportable system users is proportional to the product of the degree of frequency diversity (K) and antenna diversity (A) [9], [10]. If the number of users exceeds AK, no MIMO ZF LE can be found and detection fails. This problem can be mitigated by using the MMSE optimization criterion. In addition to providing better performance for the same amount of complexity, a MIMO MMSE LE can always be realized for an arbitrary number of system users [11]. The same is true for the MIMO MMSE DFE. It is however obvious that capacity and performance of the MMSE equalizers depend on the system diversity in some way and are negatively affected by an increase in the number of users and hence interference. For an antenna diversity system, Clark *et al.* [12] have noticed an effective diversity reduction when additional users were added. Conversely, an increase in the degree of diversity improves the system performance. Winters *et al.* [2] showed theoretically for flat fading channels with a linear antenna diversity receiver that a N user, A antenna system can null out all interferers and $A - N + 1$ path diversity improvement can be achieved by each of the users. They verified through simulations that this result also holds in frequency selective environments. Balaban and Salz [13] investigated the impact of dual antenna diversity on the performance of a single user system. It was found that a second diversity branch improved the BER and outage probability by one to two orders of magnitude. The above authors have considered exclusively antenna diversity systems with a relatively low degree of diversity and a low number of supportable users. For combined frequency/antenna diversity systems, simulation results [14], [15] indicate the same general effect that an increased amount of frequency and antenna diversity improves the system performance and capacity. It seems, however, that more detailed studies have not been published. Especially the interrelationship among system capacity, performance and the degree of diversity is not completely understood yet. In addition, little knowledge exists about the performance of the MIMO MMSE equalizers in situations when a zero-forcing LE does not exist (which we refer to as *overpopulated*). Our paper tries to provide more detailed insight into these complicated issues, showing comprehensive results for the LE and DFE in overpopulated systems. Special attention is dedicated to a comparison between LE and DFE. It is shown that the system performance of the LE depends critically on the user population and the degree of diversity. In particular, despite the existence of a unique MMSE LE, we show that the performance becomes unacceptable if N exceeds AK. For the MIMO MMSE DFE, however, we found satisfactory performance in some cases when $N > AK$. This important result has been verified through semi-analytical simulations.

In our description of the system model, we unify the concepts of spread spectrum (frequency diversity) and input (antenna) diversity. We show that a system with processing gain K and A receiver inputs provides effectively $U_{\text{div}} = AK$ parallel diversity channels. The mathematical treatment shows that there is no conceptual difference between frequency and antenna diversity. Both lead, in a similar manner, to an increase in the number of diversity channels.

It is well known that there exists a unique relationship between the signal to interference and noise ratio (SINR) and the MMSE of the single-input single-output MMSE LE and DFE [16]. We provide a proof that the same relationship holds also for both the MIMO MMSE LE and DFE. This enables us to apply the upper BER bound of Foschini *et al.* [17] and Saltzberg [18] to the MIMO equalizers investigated.

The paper is organized as follows. In Section II, the system model is introduced. We review the optimum MIMO MMSE LE and DFE in Section III. Section IV contains the derivation of an upper BER bound and expressions for the system capacity. Numerical results are shown in Section V.

II. System Model

The complex baseband notation is used to describe the system. All signals and impulse responses are in general complex functions. For convenience, let us define the set of integer numbers $\mathcal{I}_N = \{1, 2, \ldots, N\}$. Accordingly, $\mathcal{I}_A$ and $\mathcal{I}_K$ describe the set of integer numbers between 1 and A and 1 and K, respectively.

Consider the reverse link of an asynchronous spread spectrum multiuser system with N users sharing the same bandwidth, as shown in Figure 1. The users transmit data sequences a_i ($i \in \mathcal{I}_N$), which consist of symbols drawn from a finite alpha-

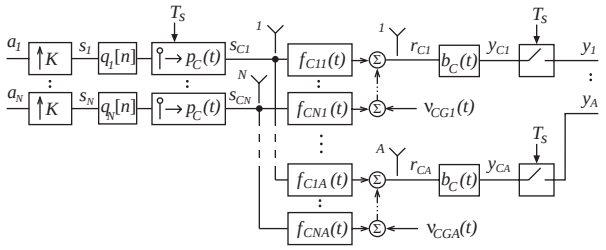

Fig. 1. System model.

bet of complex numbers ($a_i[n] \in \mathcal{A}_i$). The random variables $a_i[n]$ are assumed to have zero mean and variance

$$\mathcal{E}_{a,i} = E[|a_i[n]|^2] \tag{1}$$

where 'E' denotes the expectation operator. The symbol period is T seconds for all users. Each user is assigned a signature waveform

$$\varphi_{Ci}(t) = \sum_{m=0}^{M_i-1} q_i[m] p_C(t - mT_s) \tag{2}$$

where q_i is the spreading code of length M_i samples, $p_C(t)$ is the chip pulse shape and $T_s = T/K$ is the chip or sampling period. The spreading factor (processing gain) K is an integer number greater than or equal to 1. Note that we do not place any restrictions on the value of M_i, which may be smaller or even larger than K [19]. In addition, the samples of q_i are chosen from the set of complex numbers ($q_i[m] \in \mathcal{C}$).

The base station receives the signals at A different antennas. Let us define the overall channel waveform between user i and the l-th base antenna ($i \in \mathcal{I}_N,\ l \in \mathcal{I}_A$):

$$\psi_{Cil}(t) = \int_{-\infty}^{\infty} \varphi_{Ci}(\tau) f_{Cil}(t - \tau)\, d\tau \tag{3}$$

where f_{Cil} denotes the channel impulse response between user i and the l-th base antenna. The signal received at antenna l is

$$r_{Cl}(t) = \sum_{i=1}^{N} \sum_{n=-\infty}^{\infty} a_i[n] \psi_{Cil}(t - nT) + \nu_{CGl}(t) \tag{4}$$

where the ν_{CGl} ($l \in \mathcal{I}_A$) are mutually independent, complex additive white Gaussian noise (AWGN) signals with zero mean and a two-sided power spectral density N_0. The received signals are passed through a lowpass filter b_C, which removes high frequency interference and noise. Define the *combined channel* as

$$x_{Cil}(t) = \int_{-\infty}^{\infty} \psi_{Cil}(\tau) b_C(t - \tau)\, d\tau. \tag{5}$$

The filtered signal before sampling is then given by

$$y_{Cl}(t) = \sum_{i=1}^{N} \sum_{n=-\infty}^{\infty} a_i[n] x_{Cil}(t - nT) + \nu_{Cl}(t) \tag{6}$$

where

$$\nu_{Cl}(t) = \int_{-\infty}^{\infty} \nu_{CGl}(\tau) b_C(t - \tau)\, d\tau \tag{7}$$

is the colored thermal noise after lowpass filtering. Each signal y_{Cl} is sampled at a rate $1/T_s$, fed into an equalizer with A inputs and N outputs, and a decision is made by a nonlinear device. The final output signals $\hat{a}_k$ ($k \in \mathcal{I}_N$) are quantized estimates of the input sequences a_i. Both the input and output signals belong to the same finite alphabet ($\hat{a}_k[n] \in \mathcal{A}_k$).

For mathematical tractability, we introduce a discrete-time model that is completely equivalent to the system described above. This is done by defining the K-times upsampled input sequence $s_i[n]$ as

$$s_i[Kn + m] = \begin{cases} a_i[n] & \text{for } m = 0 \\ 0 & \text{for } m = 1, 2, \ldots, K-1 \end{cases}. \tag{8}$$

In addition, the equivalent discrete-time combined channel is

$$x_{il}[n] = T_s x_{Cil}(nT_s). \tag{9}$$

At the l-th branch of the receiver, the sampled signal $y_l[n] = y_{Cl}(nT_s)$ may be expressed in the form

$$y_l[n] = \sum_{i=1}^{N} s_i[n] \star x_{il}[n] + \nu_l[n] \tag{10}$$

where '$\star$' is the convolution operator and ν_l is the sampled noise signal $\nu_l[n] = \nu_{Cl}(nT_s)$.

Let us now assume that each signal $y_l[n]$ is followed by a $(1 : K)$ serial to parallel demultiplexer. The demultiplexer outputs are

$$y_l^m[n] = y_l[Kn + m - 1] \tag{11}$$

where m denotes the number of the demultiplexer output ($m \in \mathcal{I}_K$). Note that the time duration between consecutive samples of y_l is T_s while the sample period of the sequences y_l^m is equal to the symbol period $T = KT_s$ if the system is operating in real time. Substituting Equation (10) into (11), we obtain with Eqn. (8) after a few steps

$$y_l^m[n] = \sum_{i=1}^{N} a_i[n] \star x_{il}^m[n] + \nu_l^m[n]. \tag{12}$$

where x_{il}^m and ν_l^m are given by

$$x_{il}^m[n] = x_{il}[Kn + m - 1] \tag{13}$$
$$\nu_l^m[n] = \nu_l[Kn + m - 1]. \tag{14}$$

Let us now describe the system in vector form. The input signal vector is defined as

$$\boldsymbol{a} = [a_1, a_2, \ldots, a_N]. \tag{15}$$

The equalizer input and noise signal of receive antenna l are given by

$$\boldsymbol{y}_l = [y_l^1, y_l^2, \ldots, y_l^K] \tag{16}$$
$$\boldsymbol{\nu}_l = [\nu_l^1, \nu_l^2, \ldots, \nu_l^K]. \tag{17}$$

The combined channel matrix for the l-th receiver input shall be given by

$$\boldsymbol{X}_l = \begin{bmatrix} x_{1l}^1 & x_{1l}^2 & \ldots & x_{1l}^K \\ x_{2l}^1 & x_{2l}^2 & \ldots & x_{2l}^K \\ \vdots & \vdots & \ddots & \vdots \\ x_{Nl}^1 & x_{Nl}^2 & \ldots & x_{Nl}^K \end{bmatrix}. \tag{18}$$

The system analysis is performed using the D-transform which is defined by

$$\boldsymbol{V}(D) = \sum_{n=-\infty}^{\infty} \boldsymbol{V}[n] D^n \tag{19}$$

where $\boldsymbol{V}$ may be an arbitrary dimensional matrix or vector.

In the D-domain, the signal at the l-th receiver branch can then be expressed as $\boldsymbol{y}_l(D) = \boldsymbol{a}(D)\boldsymbol{X}_l(D) + \boldsymbol{\nu}_l(D)$. Let us now define the overall received signal, noise signal and channel matrix as

$$\boldsymbol{y} = [\boldsymbol{y}_1, \boldsymbol{y}_2, \ldots, \boldsymbol{y}_A] \tag{20}$$
$$\boldsymbol{\nu} = [\boldsymbol{\nu}_1, \boldsymbol{\nu}_2, \ldots, \boldsymbol{\nu}_A] \tag{21}$$
$$\boldsymbol{X} = [\boldsymbol{X}_1, \boldsymbol{X}_2, \ldots, \boldsymbol{X}_A]. \tag{22}$$

Thus, the overall received signal can be expressed as

$$\boldsymbol{y}(D) = \boldsymbol{a}(D)\boldsymbol{X}(D) + \boldsymbol{\nu}(D). \tag{23}$$

A. Diversity

CCI/ISI cancellation and equalization relies on a sufficient degree of diversity in the transmitted signals. This diversity is introduced into the investigated system by a combination of antenna diversity and frequency diversity. Antenna diversity is realized by receiving the signals at $A > 1$ antennas at the base station. Frequency diversity is obtained by spreading the transmitted signals by a factor of $K > 1$. If the symbol period of the transmitted signals is T, the minimum required double-sided bandwidth (Nyquist criterion) is $B_T = 1/T$. After spreading, the signal bandwidth is K/T. The *total degree of diversity* is defined as the product of antenna and frequency diversity:

$$U_{\text{div}} = AK. \tag{24}$$

As long as no more than U_{div} users are present, the system is referred to as *well populated*. If the number of users N exceeds the total degree of diversity, we will call the system *overpopulated*.

The basis of the Definition (24) is the fact that the system may be viewed as one with AK independent channel outputs and receiver inputs. Hence, there are exactly U_{div} diversity channels in the system. This can be verified mathematically through Equation (23): the overall received signal vector $\boldsymbol{y}$ has AK components. Each component can be interpreted as a separate, independent input signal to the equalizer.

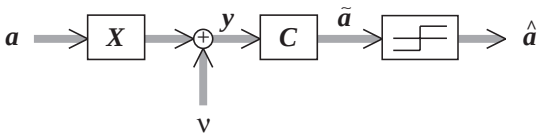

(a) linear equalizer (LE)

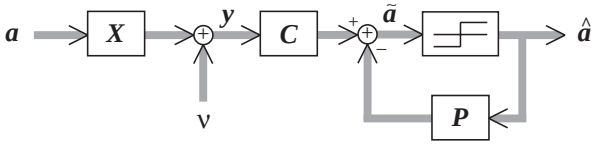

(b) decision-feedback equalizer (DFE)

Fig. 2. System model including (a) a linear equalizer (LE), and (b) a decision-feedback equalizer (DFE).

III. Optimal MMSE Equalizers and MMSE Performance

The optimal linear and DFE receiver structures for the MMSE criterion are discussed in this section. The vector system models including a linear and decision-feedback equalizer are shown in Figures 2 (a) and (b), respectively. A linear transformation $\boldsymbol{C}(D)$ is applied to the overall received signal $\boldsymbol{y}(D)$ (Eqn. (23)). This constitutes the feedforward filter of both LE and DFE. It has been shown, [20], [21], [22], that the optimal MMSE forward filter is

given by

$$\boldsymbol{C}(D) = \boldsymbol{S}_\nu^{-1}(D)\boldsymbol{X}^H(D^{-*})\boldsymbol{L}(D) \tag{25}$$

where $\boldsymbol{S}_\nu(D)$ is the power spectrum of the noise $\boldsymbol{\nu}$ and 'H' denotes the conjugate transpose of a matrix. The superscript '$-*$' shall be interpreted in the sense $D^{-*} = (D^{-1})^*$, where '$*$' and '-1' denote complex conjugation and inversion, respectively. This shows that the optimum forward filter consists of a noise-whitening matched filter $\boldsymbol{S}_\nu^{-1}(D)$ followed by a channel matched filter $\boldsymbol{X}^H(D^{-*})$ and a linear transformation $\boldsymbol{L}(D)$. For the LE, $\boldsymbol{L}(D)$ is given by [8]

$$\boldsymbol{L}_{\text{le}}(D) = [\boldsymbol{S}_x(D) + \boldsymbol{S}_a^{-1}(D)]^{-1} \tag{26}$$

$$\boldsymbol{S}_x(D) = \boldsymbol{X}(D)\boldsymbol{S}_\nu^{-1}(D)\boldsymbol{X}^H(D^{-*}) \tag{27}$$

where $\boldsymbol{S}_a(D)$ is the power spectrum of the input signal $\boldsymbol{a}$.

The optimum forward and feedback filters for the DFE have been derived by Duel-Hallen [8] and Vandendorpe *et al.* [22]. Let us define the spectrum

$$\boldsymbol{Q}(D) = \boldsymbol{S}_x(D) + \boldsymbol{S}_a^{-1}(D). \tag{28}$$

This spectrum may be factored into [23]

$$\boldsymbol{Q}(D) = \boldsymbol{\Psi}(D)\boldsymbol{G}^{-1}\boldsymbol{\Psi}^H(D^{-*}) \tag{29}$$

where $\boldsymbol{\Psi}(D)$ is a causal and stable matrix with $\boldsymbol{\Psi}(D) = \boldsymbol{\Psi}[0] + \boldsymbol{\Psi}[1]D + \boldsymbol{\Psi}[2]D^2 + \ldots$. The DC-component $\boldsymbol{\Psi}[0]$ is constrained to be an upper triangular matrix with ones on the main diagonal. $\boldsymbol{G}^{-1}$ is a diagonal matrix independent on D. The optimum forward and feedback filters may then be expressed as

$$\boldsymbol{L}_{\text{dfe}}(D) = \boldsymbol{\Psi}^{-H}(D^{-*})\boldsymbol{G} \tag{30}$$

$$\boldsymbol{P}_{\text{dfe}}(D) = \boldsymbol{\Psi}(D) - \boldsymbol{I}_N \tag{31}$$

where $\boldsymbol{\Psi}^{-H}(D^{-*}) = [\boldsymbol{\Psi}^H(D^{-*})]^{-1}$.

Let the normalized minimum mean-square error (NMMSE) at the input of the k-th quantizer be

$$\sigma_k^2 = E[|e_k[n]|^2]/\mathcal{E}_{a,k} \tag{32}$$

where e_k is the k-th component of the error signal $\boldsymbol{e} = \tilde{\boldsymbol{a}} - \boldsymbol{a}$, and $\tilde{\boldsymbol{a}}$ is the input signal to the decision elements. $\boldsymbol{R}_e[m] = E[\boldsymbol{e}^H[n-m]\boldsymbol{e}[n]]$ is the cross covariance matrix of the error. The MMSE for user k is then given by the k-th diagonal element of $\boldsymbol{R}_e[0]$ and the NMMSE is

$$\sigma_k^2 = [\boldsymbol{R}_e[0]]_{kk}/\mathcal{E}_{a,k}. \tag{33}$$

$\boldsymbol{R}_e[0]$ may be calculated by

$$\boldsymbol{R}_e[0] = \int_0^1 \boldsymbol{S}_e(e^{-j2\pi\check{f}})\, d\check{f}. \tag{34}$$

where $\boldsymbol{S}_e(D)$ is the power spectrum of the error signal $\boldsymbol{e}(D)$.

Given the expressions for the channel and the optimum equalizer filters, it is easy to show that the error spectrum of the MIMO MMSE LE is equal to the transfer function of the forward filter

$$\boldsymbol{S}_{e,\text{le}}(D) = \boldsymbol{L}_{\text{le}}(D) = [\boldsymbol{S}_x(D) + \boldsymbol{S}_a^{-1}(D)]^{-1}. \tag{35}$$

On the other hand, assuming that all fed-back decisions are correct, the error spectrum of the MIMO MMSE DFE is

$$\boldsymbol{S}_{e,\text{dfe}}(D) = \boldsymbol{G}. \tag{36}$$

IV. Upper BER Bound and Capacity

In order to obtain an estimate of the system performance in terms of the bit-error rate (BER), we resort to an upper bound. For simplicity, we restrict ourselves to quadrature amplitude modulated (QAM) systems with square signal constellations (i.e. 4-, 16-, 64-QAM, ...). The inphase as well as the quadrature signal of user k are then pulse amplitude modulated with an even number L_k of signal levels each.

Without loss of generality, we may use as PAM signal levels the set of odd integer numbers

$$\pm 1, \pm 3, \ldots, \pm(L_k - 1). \tag{37}$$

Provided that the data signals are uncorrelated and equiprobable, the variance of the two real amplitude modulated signals is $\mathcal{E}_{q,k} = (L_k^2 - 1)/3$. If the quadrature and inphase components are treated as one complex signal $a_k[n]$, the number of symbols in the QAM scheme (alphabet size) will be L_k^2 and the variance of the complex input data will be

$$\mathcal{E}_{a,k} = \frac{2}{3}(L_k^2 - 1). \tag{38}$$

An upper bound for the BER of a single-input single output system was derived by Foschini *et al.* [17]; it can easily be shown that the exponent in Equation (13) of this paper [17] is identical to the signal to interference and noise ratio (SINR) divided by the variance of the input data. Using a Gray code for the the L_k^2-QAM signal constellation, the BER for the k-th user is upper bounded by

$$P_{b,k} < 2\frac{L_k - 1}{L_k}\, e^{-\Phi_k/\mathcal{E}_{a,k}} \tag{39}$$

where Φ_k is the SINR per symbol for user k at the input to the nonlinear decision device. It is straightforward to show that the above expression is also valid in the presence of co-channel interference.

In order to express the upper BER bound (39) directly in terms of the MMSE, the following relationship may be used:

$$\Phi_k = \frac{1-\sigma_k^2}{\sigma_k^2}. \tag{40}$$

This relationship is well known for the single-input single-output case [16]. In addition, it also holds for both MIMO LE and DFE when CCI is present. A proof is given in Appendix I.

Let us now derive the asymptotic capacity in bits per degree of diversity for the overall system. We start with the Saltzberg bound in Equation (39) and simplify this expression by further loosening the bound to

$$P_{b,k} < 2\, e^{-\Phi_k/\mathcal{E}_{a,k}}, \tag{41}$$

where the factor $(L_k-1)/L_k$ has been replaced by 1. Let b_k be the number of bits per symbol transmitted by user k. Using Equation (38) and $L_k^2 = 2^{b_k}$, we may solve for b_k:

$$b_k > \log_2 \left\{ \frac{\Phi_k}{\frac{2}{3}\ln\left(\frac{2}{P_{b,k}}\right)} + 1 \right\}. \tag{42}$$

Let us now define the *asymptotic capacity* as the sum over the number of bits conveyable by all system users for a desired BER $P_b = P_{b,k}\ \forall k \in \mathcal{I}_N$. Normalized by the degree of diversity, AK, a lower bound for the asymptotic capacity is given by

$$C_{\text{as}} = \frac{1}{AK} \sum_{k=1}^{N} \log_2 \left\{ \frac{\Phi_k}{\frac{2}{3}\ln\left(\frac{2}{P_b}\right)} + 1 \right\}. \tag{43}$$

It is clear that the terms in the summation of Equation (43) are in general real but not integer numbers. In practice, however, the number of transmitted bits can only be an integer number. Moreover, the square QAM schemes considered above allow only an even number of bits to be coded into a symbol. Based on this practical constraint, we define the *minimum practically achievable capacity* per degree of diversity as

$$C = \frac{1}{AK} \sum_{k=1}^{N} 2 \left\lfloor \frac{1}{2} \log_2 \left\{ \frac{\Phi_k}{\frac{2}{3}\ln\left(\frac{2}{P_b}\right)} + 1 \right\} \right\rfloor \tag{44}$$

where $\lfloor x \rfloor$ is the largest integer smaller or equal to x. Equations (39), (43) and (44) are valid without restrictions for the linear MIMO MMSE equalizer. However, this is not the case for the MIMO MMSE DFE since the effect of fed-back incorrect decisions has been neglected. In fact, under certain circumstances, error propagation has a major influence on the system capacity while in other cases it may well be justified to neglect it.

A. Matched Filter Bound

In order to evaluate the results of the MMSE equalizers, their performance is compared to the *matched filter bound*. The matched filter bound constitutes the ultimate performance and achieves the maximal receiver output SNR when no interference is present. It can be shown that the largest SNR is achieved with maximal ratio combining. The output SNR per received symbol of the maximal ratio combiner is given by

$$\Gamma_k = \frac{\mathcal{E}_{a,k}}{N_0} \sum_{l=1}^{A} \int_{-\infty}^{\infty} |\psi_{Ckl}(t)|^2 \, dt. \tag{45}$$

Note that this expression is equal to the received SNR/symbol of user k (SNR_k). The BER results in the following section are plotted against this quantity. Since interference is assumed to be absent, the noise in the output of the maximal ratio combiner is Gaussian distributed and the matched filter bound for the BER may readily be expressed in terms of the average output SNR Γ_k:

$$P_{b,k}^{(0)} = 2\frac{L_k-1}{L_k}\, Q\left(\sqrt{2\frac{\Gamma_k}{\mathcal{E}_{a,k}}}\right). \tag{46}$$

V. Numerical Results

The results presented in this section were obtained under the following ideal assumptions: Infinite length forward and (for the DFE) feedback filters, the channel impulse responses are known without error, the equalizer signals and tap weights are of infinite precision, and all decisions fed back into the DFE feedback filter are correct, i.e. the results do not include error propagation.

We considered two systems with different total degrees of diversity:

- 2×2 system (low diversity): $A = 2, K = 2, U_{\text{div}} = 4$.
- 4×4 system (high diversity): $A = 4, K = 4, U_{\text{div}} = 16$.

The low diversity system is investigated exclusively for a symbol period of $T = 50$ ns and equal energy users, i.e. it is assumed that the received energy from all users is the same ($\text{SNR} = \text{SNR}_k, \forall k \in \mathcal{I}_N$). This corresponds to a system with perfect power control. For the high diversity system, symbol periods of $T = 50$ ns and $T = 200$ ns have been chosen. In

addition to the case of equal energy users, a second scenario with different energy users is also considered. This involves a maximum difference in the received energy (*near-far ratio*) of 10 dB between the strongest and the weakest user. The energies of the users are randomly chosen within the 10 dB interval, the distribution of the random energies being uniform in that interval.

Identical fifth-order butterworth lowpass filters with a cut-off frequency $f_c = K/(2T)$ have been chosen for the analog transmit and receive filters $p_C(t)$ and $b_C(t)$. The spreading filters of all users have been set to $q_i[n] = \delta_K[n]$[1]. In other words, the filters q_i ($\forall i \in \mathcal{I}_N$) have been omitted completely. This was justified because the individual channels were strongly frequency selective and mutually uncorrelated. The use of orthogonal or other spreading filters was found to yield no improvement over the presented results.

The results have been obtained with a semi-analytical approach. Based on a statistical model for the input data, the NMMSE, equalizer output SINR and BER have been calculated analytically using the aforementioned expressions and bounds. These results have then been averaged over different radio channels drawn from an ensemble of real indoor channel impulse responses (CIR's). The CIR's have been measured in an indoor office environment at TR*Labs* [24]. The measurement system included four stationary transmit antennas and a mobile with four receive antennas. The distance between two adjacent receive antennas was one wavelength of the carrier frequency $f_{\text{car}} = 1.8$ GHz. The stationary antennas were placed in different corners of the office environment. Different impulse responses were obtained by changing the location of the mobile. Each measurement at a certain mobile location yielded four sets of four CIR's between the adjacent mobile antennas and one of the stationary antennas. The four CIR's belonging to one set had the same large scale propagation characteristics because the distances between a certain stationary antenna and each of the four mobile antennas were practically the same. A total of 2044 sets or 8176 CIR's had been obtained. The bandwidth of the measured CIR's was approximately 120 MHz. It was found that the CIR's had an RMS delay spread distribution with a mean of 40.4 ns and a standard deviation of 9.2 ns [24]. These values indicate that the channels are frequency selective for the chosen symbol periods of $T = 50$ ns and $T = 200$ ns. A considerable amount of ISI and CCI over several symbols

[1] $\delta_K[n] = \begin{cases} 1; & n = 0 \\ 0; & n \neq 0. \end{cases}$

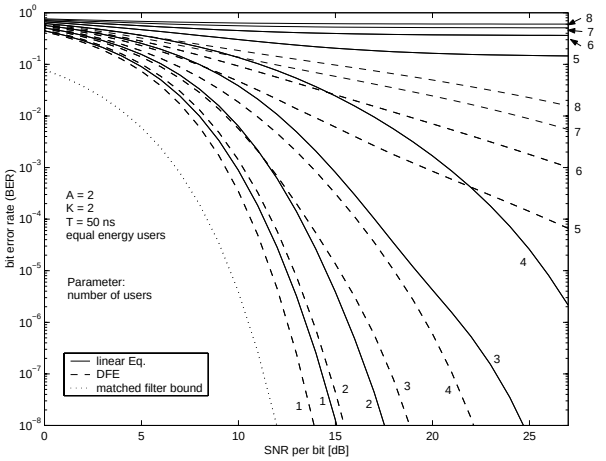

Fig. 3. Upper BER bound versus average received SNR for 2×2, $T = 50$ ns systems with a different number of equal energy users.

can thus be expected.

The reverse link of the system has been simulated by randomly selecting M out of 2044 CIR sets and assigning each to one of M users[2]. These users have been divided into several groups of N portables for which the theoretical NMMSE's, BER bounds, outage probabilities and capacities have been calculated. This procedure has been repeated 100 times for each value of N with different CIR sets.

Let us start with an investigation of upper BER bounds, averaged over all users and trials, for the MIMO MMSE LE and DFE. Figure 3 displays the BER versus the received SNR for the 2×2 system. There are 8 curves for both equalizers, each one for a different system population ($N = 1, 2, \ldots, 8$). It can be seen that the DFE performs in all cases considerably better than the linear equalizer. The LE displays the characteristic waterfall-like shape of the BER for $N = 1, 2, 3$ users. For 4 users the BER also seems to decrease, however, a much higher input SNR is required for low BER values. For more than 4 users, the curves of the LE show an irreducible BER floor. This is explained by the fact that the total degree of diversity in this system is $U_{\text{div}} = 4$, allowing up to 4 users with reliable performance if a LE is employed. Figure 4 shows the corresponding results for the 4×4 system. Remarkable is the performance of the DFE with 20 users, i.e. 4 more users than the total degree of diversity. Average BER's of less than 10^{-6} can be achieved for received SNR's per bit greater than 27 dB. This means that the DFE performs well even in overpopulated systems. Error propagation effects have most probably no qualita-

[2] Depending on the investigated scenario, M took on the values 8, 20 and 30.

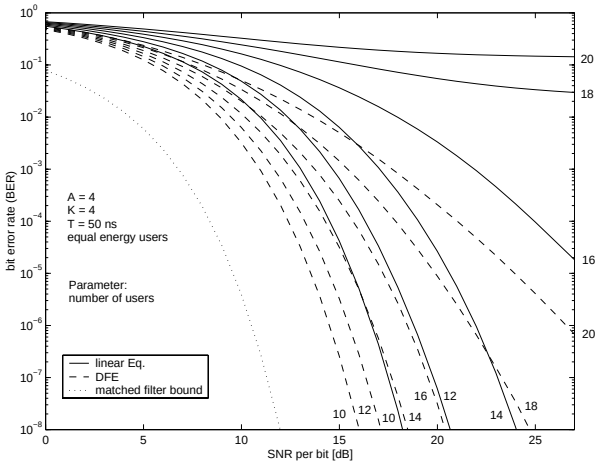

Fig. 4. Upper BER bound versus average received SNR for 4×4, $T = 50$ ns systems with a different number of equal energy users.

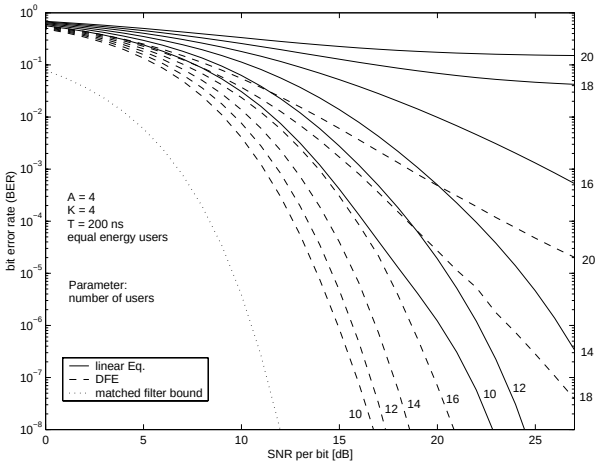

Fig. 5. Upper BER bound versus average received SNR for 4×4, $T = 200$ ns systems with a different number of equal energy users.

tive influence on this result since the variation of all calculated BER's, including the ones from the worst users, is relatively small around the average values shown in the figures. Hence, the performance of all system users is good, which makes the occurrence of errors relatively rare. Under this circumstance, it has been shown that error propagation does not lead to pathological situations but only to an overall performance loss of approximately 2 dB [16].

Results for an identical 4×4 system except a longer symbol period of $T = 200$ ns are given in Figure 5. The lower amount of "implicit" diversity [12], [25] leads to a worse performance of the LE compared to the $T = 50$ ns case for all user populations shown while the results of the DFE seem to be degraded only in overpopulated scenarios.

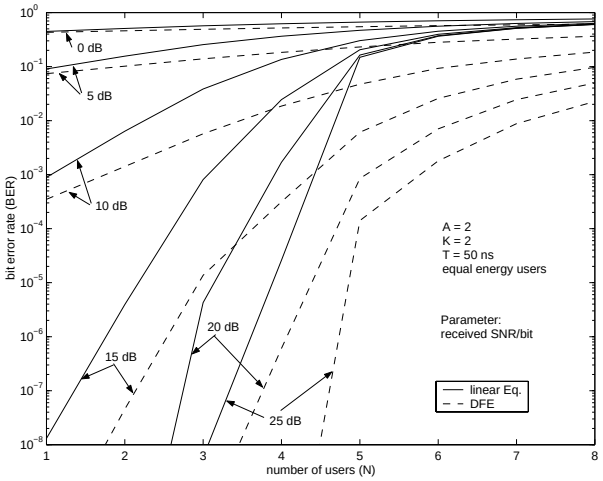

Fig. 6. Upper BER bound versus number of users for 2×2, $T = 50$ ns systems with different average received SNR's and equal energy users.

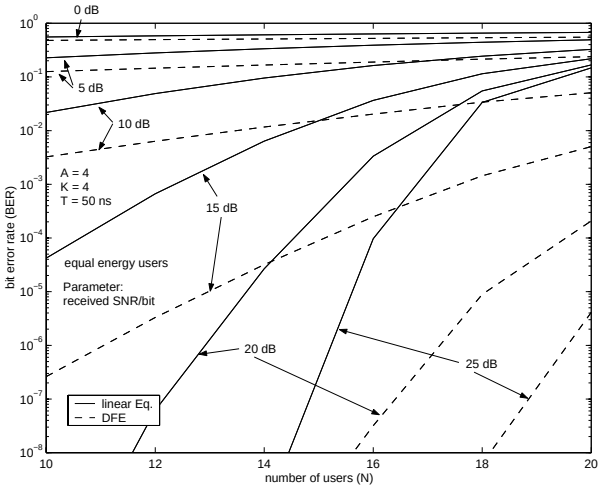

Fig. 7. Upper BER bound versus number of users for 4×4, $T = 50$ ns systems with different average received SNR's and equal energy users.

The next two Figures 6 and 7 show the average BER versus the number of users with the received SNR/bit as parameter. It can be observed that the DFE is able to support consistently a larger number of users for the same error probability than the LE. These figures also confirm that a larger received SNR does not have much effect on the performance of the LE when the system is overpopulated. On the other hand, the DFE has the potential to achieve a distinctly better performance gain by increasing the SNR in situations with many users.

The next results measure the system performance in terms of the outage probability. We assume an outage condition if the Saltzberg upper bound BER of an individual user is larger than 10^{-4}. The outage

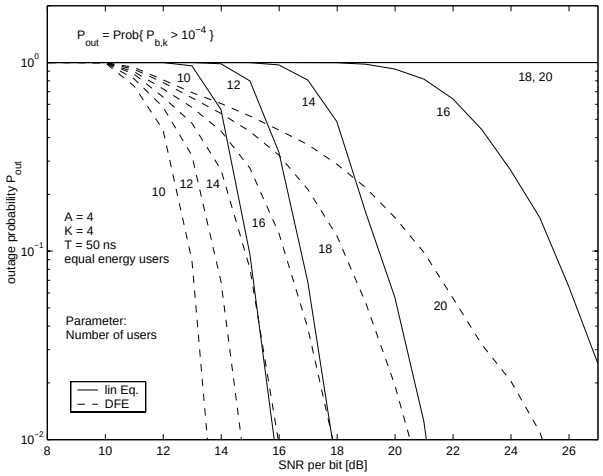

Fig. 8. Estimated outage probability versus average received SNR for 4×4, $T = 50$ ns systems with a different number of equal energy users.

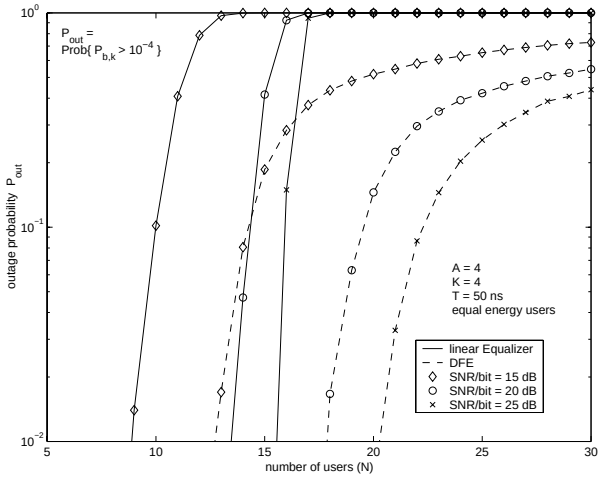

Fig. 9. Estimated outage probability versus number of users for 4×4, $T = 50$ ns systems with different average received SNR's and equal energy users.

probability is then

$$P_{\text{out}} = \text{Prob}\{P_{b,k} > 10^{-4}\}, \tag{47}$$

where $P_{b,k}$ is the upper bound of the BER. For the transfer of data, a raw BER of 10^{-4} before coding is generally considered appropriate. An estimate of the outage probability is calculated with

$$\hat{P}_{\text{out}} = N_{\text{out}}/N_{\text{tot}} \tag{48}$$

where N_{out} is the number of users whose upper bound BER exceeded 10^{-4} and $N_{\text{tot}} = 2000$ is the total number of users for which the BER bound was computed.

The estimated outage probability versus the received SNR/bit for the 4×4 system with $T = 50$ ns is shown in Figure 8. As can be seen, the LE may achieve outage probabilities of less than 1% for 10, 12 and 14 users. For $N = 16$, a considerably higher SNR is necessary in order to obtain low outage values. When the number of users is larger than the total degree of diversity, the outage probability does not decrease below 100% over the whole SNR range displayed. The DFE may achieve low outage probabilities for $N < 16$. Even if the number of users becomes larger than 16, small outage probabilities can be obtained in low noise environments. This example provides further evidence for the superiority of the DFE especially in highly populated and overpopulated systems.

The next two figures plot the outage probability over the number of system users. In the equal energy user case (Figure 9), between 4 and 5 more users can be supported for the same outage probability if a DFE receiver is employed instead of a LE. This result was found to be independent of the received SNR/bit. It also seems as if the DFE may allow a significant portion of the users (about 40% for 25 dB SNR/bit) to communicate reliably even if the number of users is almost twice the total degree of diversity. In this case, however, the effect of incorrect decisions must be taken into account. The users which are in an outage condition may cause a considerable amount of errors. This affects, in turn, also the better users through the decision-feedback loop. Since the number of users which perform poorly is large and since their error probability might be high, the negligence of error propagation leads in Figures 9 and 10 to overly optimistic results for $N \gg U_{\text{div}}$. Figure 10 considers the case of users received with different SNR's (near-far effect). The near-far ratio was set to 10 dB. Compared to the equal energy case, the performance suffers between dramatically for low SNR's of 15 dB to mildly at higher SNR's. The advantage of a DFE over a LE seems to be hardly affected. Overall, the near-far effect did not cause problems for the equalizers.

The final investigation considers the system capacity. The average asymptotic capacity (43) of the 4×4, 50 ns system with equal energy users is shown in Figure 11 for a desired minimum BER probability of $P_b = 10^{-4}$. A clear difference in the behavior of LE and DFE can be noticed. The asymptotic capacity of the LE has a distinct maximum for 12 users and decreases for increasing N. In largely overpopulated systems, the asymptotic capacity is not dependent on the received SNR. On the other hand, the asymptotic capacity of the DFE increases almost linearly for small N. After the maximum is reached for

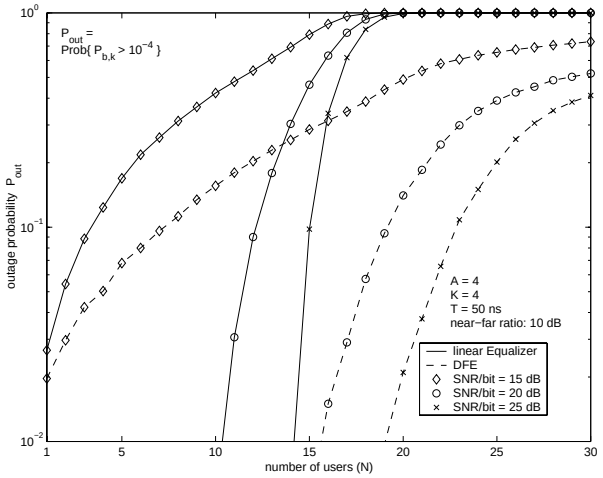

Fig. 10. Estimated outage probability versus number of users for 4×4, $T = 50$ ns systems with different average received SNR's a near-far ratio of 10 dB.

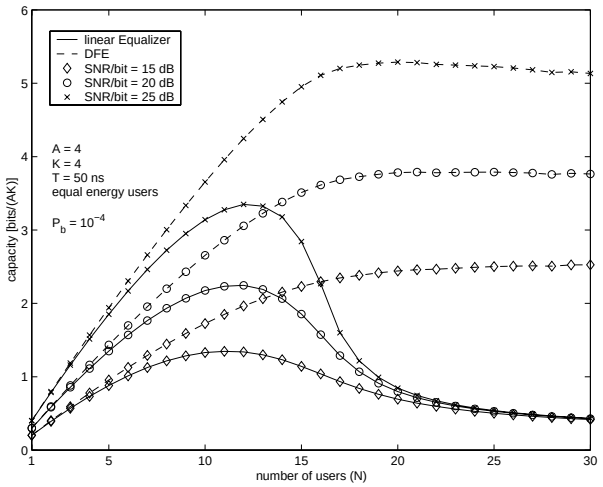

Fig. 11. Asymptotic capacity versus number of users for 4×4, $T = 50$ ns systems with different average received SNR's and equal energy users.

approximately 19 users, the capacity decreases only marginally. The asymptotic capacity of the DFE for large N still depends on the received SNR. Almost identical results for the asymptotic capacity were found for users received with unequal energies.

A more realistic performance measure is the practically achievable capacity (44). Figure 12 shows a lower bound of this quantity for the same system as above. The differences are obvious. For small values of N, the capacity curves increase linearly with three different slopes, each corresponding to a modulation scheme of 4-QAM, 16-QAM and 36-QAM, respectively. Some curves have local maxima. Independent of the received SNR, the capacity of the

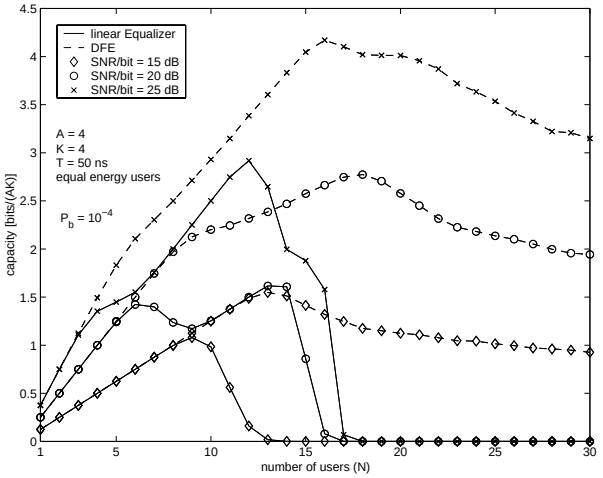

Fig. 12. Practical capacity versus number of users for 4×4, $T = 50$ ns systems with different average received SNR's and equal energy users.

LE is zero in overpopulated scenarios. The curves of the DFE have to be treated with caution for large N because error propagation is neglected. In all cases, the DFE achieves its capacity maximum at larger N than the LE.

Interestingly, in contrast to the asymptotic capacity, the practically achievable capacity results are quite different for the equal and unequal energy user cases. An example with a near-far ratio of 10 dB is displayed in Figure 13. The curves resemble more those of the asymptotic capacity and have only one maximum. For the DFE, the capacity values at the maxima are approximately the same for both equal and unequal energy scenarios. The practically achievable capacity of the LE decreases slightly for increasing near-far ratios. Overall, both DFE and LE suffer only small capacity losses due to the near-far effect.

VI. Conclusion

The performance of equalizers for multiuser systems was investigated in terms of the BER, outage probability and capacity. We found that the decision-feedback equalizer (DFE) may achieve sufficiently good results in systems where the number of users exceeds the total degree of diversity, while a linear equalizer (LE) always performed unsatisfactorily under these circumstances. In situations when the number of users was distinctly smaller than the total degree of diversity, the DFE did not perform significantly better. With growing user populations, the performance advantage of the DFE was increasing. Therefore, the LE may be a good choice for systems with low user populations since it is less

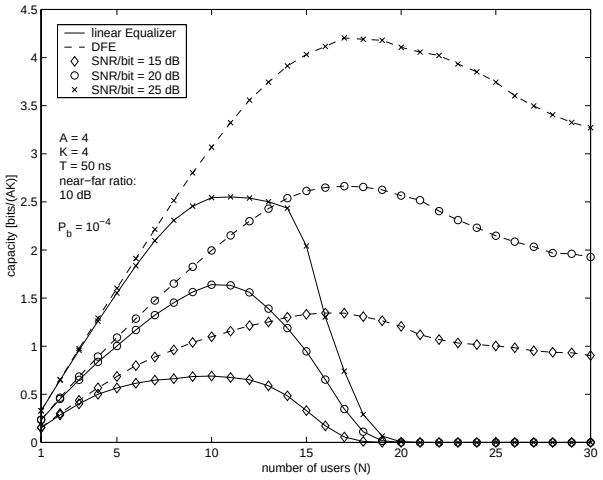

Fig. 13. Practical capacity versus number of users for 4×4, $T = 50$ ns systems with different average received SNR's and a near-far ratio of 10 dB.

complex than the DFE. For densely populated and especially overpopulated systems, only a DFE may offer reliable communication quality. Both equalizer types proved to be robust in near-far scenarios.

Acknowledgments

This work was supported by research grants and graduate scholarships from the Telecommunications Research Laboratories (TR*Labs*), the Natural Sciences and Engineering Research Council of Canada (NSERC) and The University of Calgary.

Appendix

I. Relationship between SINR and normalized MMSE

Denote the output signal of the equalizer forward filter by $\boldsymbol{u}$. We obtain according to Section III

$$\boldsymbol{u}(D) = \boldsymbol{a}(D)\boldsymbol{H}(D) + \boldsymbol{\zeta}(D) \tag{49}$$

where

$$\boldsymbol{H}(D) = \boldsymbol{S}_x(D)\boldsymbol{L}(D) \tag{50}$$

$$\boldsymbol{\zeta}(D) = \boldsymbol{\nu}(D)\boldsymbol{S}_\nu^{-1}(D)\boldsymbol{X}^H(D^{-*})\boldsymbol{L}(D) \tag{51}$$

are the total transfer function from the data input to the equatizer output and the noise signal at the equalizer output, respectively. Let $\boldsymbol{H}[n]$ and $\boldsymbol{\zeta}[n]$ be the inverse D-transform of $\boldsymbol{H}(D)$ and $\boldsymbol{\zeta}(D)$, respectively. With $h_{ik} = [\boldsymbol{H}]_{ik}$ and $\zeta_k = [\boldsymbol{\zeta}]_k$ $(i, k \in \mathcal{I}_N)$, the input to the k-th decision element may be expressed as

$$\tilde{a}_k[n] = a_k[n]h_{kk}[0] + \sum_{i=1}^{N} \sum_{m \notin S_i} a_i[n-m]h_{ik}[m] + \zeta_k[n] \tag{52}$$

where the set S_i includes the interference from user i that is cancelled by the decision-feedback loop. Since the complex baseband notation is used to describe the system, the impulse responses h_{ik} can be expressed in terms of their real and imaginary parts

$$h_{ik}[n] = \mu_{ik}[n] + j\gamma_{ik}[n]. \tag{53}$$

The signal component at the input to the decision element is thus $a_k[n]\mu_{kk}[0]$ and the average signal energy is

$$\mathcal{E}_{s,k} = \mathcal{E}_{a,k}\mu_{kk}^2[0]. \tag{54}$$

On the other hand, the noise energy is

$$\mathcal{E}_{n,k} = E\left[|\tilde{a}_k[n] - a_k[n]\mu_{kk}[0]|^2\right]. \tag{55}$$

It is assumed that the input sequences $a_k[n]$ and $a_i[m]$ are uncorrelated for $k \neq i$ or $n \neq m$ Furthermore, the noise and input sequences are uncorrelated. Considering Equation (52), it is then easy to show that

$$E\left[a_k^*[n]\tilde{a}_k[n]\right] = \mathcal{E}_{a,k}h_{kk}[0]. \tag{56}$$

Expanding Equation (55) by expressing it exclusively in terms of the expectations

$$E\left[|\tilde{a}_k[n] - a_k[n]|^2\right] = \mathcal{E}_{a,k}\sigma_k^2 \tag{57}$$

$$E\left[|a_k[n]|^2\right] = \mathcal{E}_{a,k} \tag{58}$$

and $E\left[a_k^*[n]\tilde{a}_k[n]\right]$ (56) yields

$$\mathcal{E}_{n,k} = \mathcal{E}_{a,k}\left[\sigma_k^2 - (1 - \mu_{kk}[0])^2\right]. \tag{59}$$

It is proven subsequently for both the MIMO MMSE LE and DFE that the NMMSE and the *bias coefficients* $\mu_{kk}[0]$ are related through

$$\mu_{kk}[0] = 1 - \sigma_k^2, \quad \forall k \in \mathcal{I}_N. \tag{60}$$

Substituting this result into Equations (54) and (59) yields the sought after relationship between SINR $\Phi_k = \mathcal{E}_{s,k}/\mathcal{E}_{n,k}$ and NMMSE σ_k^2:

$$\Phi_k = \frac{1 - \sigma_k^2}{\sigma_k^2}. \tag{61}$$

A. Relation between the NMMSE and the bias coefficient for the LE

The expression for the optimum MIMO MMSE LE is given in Equation (26). Consequently, the total transfer function from the data input to the equalizer output is

$$\begin{aligned}\boldsymbol{H}(D) &= \boldsymbol{S}_x(D)\boldsymbol{L}_{\text{le}}(D) \\ &= \boldsymbol{I}_N - \boldsymbol{S}_a^{-1}(D)[\boldsymbol{S}_x(D) + \boldsymbol{S}_a^{-1}(D)]^{-1}. \quad (62)\end{aligned}$$

Since the transmitted data sequences are mutually uncorrelated, the spectrum of the input data $\boldsymbol{S}_a(D)$ becomes a constant diagonal matrix whose k-th diagonal element is $[\boldsymbol{S}_a(D)]_{kk} = \mathcal{E}_{a,k}$. It is shown in Section III that the NMMSE for user k, σ_k^2, is given by the k-th diagonal element of the matrix

$$\boldsymbol{S}_a^{-1}\boldsymbol{R}_e[0] = \boldsymbol{S}_a^{-1}\int_0^1 [\boldsymbol{S}_x(e^{-j2\pi\check{f}}) + \boldsymbol{S}_a^{-1}]^{-1}\, d\check{f}. \quad (63)$$

The bias coefficient may be obtained from the overall system transfer function $\boldsymbol{H}(D)$. The system impulse response at time $n = 0$ is given by

$$\boldsymbol{H}[0] = \int_0^1 \boldsymbol{H}(e^{-j2\pi\check{f}})d\check{f} \quad (64)$$

and $h_{kk}[0] = \mu_{kk}[0] + j\gamma_{kk}[0]$ is the k-th diagonal element of $\boldsymbol{H}[0]$. Substituting Equation (62) into (64) and using (63) we obtain

$$\boldsymbol{H}[0] = \boldsymbol{I}_N - \boldsymbol{S}_a^{-1}\boldsymbol{R}_e[0]. \quad (65)$$

$\boldsymbol{S}_a^{-1}$ is a diagonal matrix with real elements. In addition, the diagonal elements of the cross covariance matrix $\boldsymbol{R}_e[0]$ are also real. Thus, all diagonal elements of $\boldsymbol{H}[0]$ are real, i.e. $h_{kk}[0] = \mu_{kk}[0]$. Since the k-th diagonal element of the matrix $\boldsymbol{S}_a^{-1}\boldsymbol{R}_e[0]$ is equal to the NMMSE for user k, it can be concluded that

$$\mu_{kk}[0] = 1 - \sigma_k^2, \quad \forall k \in \mathcal{I}_N. \quad (66)$$

B. Relation between the NMMSE and the bias coefficient for the DFE

Let us again start with the total system transfer function from the input to the output of the DFE forward filter

$$\boldsymbol{H}(D) = \boldsymbol{S}_x(D)\boldsymbol{L}_{\text{dfe}}(D). \quad (67)$$

This equation may be manipulated using Equations (28), (29), and (30) such that

$$\boldsymbol{H}(D) = \boldsymbol{\Psi}(D) - \boldsymbol{S}_a^{-1}\boldsymbol{\Psi}^{-H}(D^{-*})\boldsymbol{G}. \quad (68)$$

The total system impulse response at the time $n = 0$ is then

$$\begin{aligned}\boldsymbol{H}[0] &= \int_0^1 \boldsymbol{H}(e^{-j2\pi\check{f}})d\check{f} \\ &= \boldsymbol{\Psi}[0] - \boldsymbol{S}_a^{-1}\boldsymbol{\Psi}^{-H}[0]\boldsymbol{G}, \quad (69)\end{aligned}$$

where $\boldsymbol{\Psi}^{-H}[0] = \int_0^1 [\boldsymbol{\Psi}^H(e^{-j2\pi\check{f}})]^{-1}d\check{f}$. Note that $\boldsymbol{\Psi}(D) = \boldsymbol{\Psi}[0] + \boldsymbol{\Psi}[1]D + \boldsymbol{\Psi}[2]D^2 + \ldots$ is causal, and $\boldsymbol{\Psi}[0]$ is an upper triangular matrix with ones on the main diagonal. Thus, $\boldsymbol{\Psi}^H(D^{-*})$ is anticausal and may be written as

$$\boldsymbol{\Psi}^H(D^{-*}) = \boldsymbol{I}_N + \boldsymbol{\Theta}(D), \quad (70)$$

where $\boldsymbol{\Theta}(D)$ is also anticausal with a DC-coefficient matrix $\boldsymbol{\Theta}[0]$ that is lower triangular with zeros on the main diagonal. Based on Equation (70), the inverse of $\boldsymbol{\Psi}^H(D^{-*})$ can be developed into a series:

$$\left[\boldsymbol{\Psi}^H(D^{-*})\right]^{-1} = \boldsymbol{I}_N + \sum_{\nu=1}^{\infty}(-1)^\nu\boldsymbol{\Theta}^\nu(D). \quad (71)$$

Since $\boldsymbol{\Theta}(D)$ is anticausal and has a lower triangular DC-matrix with zeros on the main diagonal, $\boldsymbol{\Theta}^\nu(D) = [\boldsymbol{\Theta}(D)]^\nu$ is also anticausal and has a lower triangular DC-matrix with zeros on the main diagonal. As a result, the DC coefficient matrix $\boldsymbol{\Psi}^{-H}[0]$ of $[\boldsymbol{\Psi}^H(D^{-*})]^{-1}$ is lower triangular with ones on the main diagonal.

Let us now continue with some observations on Equation (69). Firstly, we note that the k-th diagonal element of $\boldsymbol{H}[0]$ is equal to $h_{kk}[0] = \mu_{kk}[0] + j\gamma_{kk}[0]$. Secondly, both $\boldsymbol{S}_a^{-1}$ and $\boldsymbol{G}$ are diagonal matrices with real elements. Thirdly, both $\boldsymbol{\Psi}[0]$ and $\boldsymbol{\Psi}^{-H}[0]$ have ones on the main diagonal. As a result, $h_{kk}[0]$ is given by

$$h_{kk}[0] = 1 - \mathcal{E}_{a,k}^{-1}[\boldsymbol{G}]_{kk}, \quad (72)$$

where $[\boldsymbol{G}]_{kk}$ is the k-th diagonal element of $\boldsymbol{G}$. Since the right hand side of the above equation is real, we find $h_{kk}[0] = \mu_{kk}[0]$. It is also known from Section III that $[\boldsymbol{G}]_{kk}$ is equal to the (unnormalized) MMSE. Thus, the bias coefficient is given by

$$\mu_{kk}[0] = 1 - \sigma_k^2, \quad \forall k \in \mathcal{I}_N. \quad (73)$$

References

[1] Jack H. Winters, "Optimum combining for indoor radio systems with multiple users," *IEEE Trans. Commun.*, vol. COM-35, no. 11, pp. 1222–1230, Nov. 1987.

[2] Jack H. Winters, Jack Salz, and Richard D. Gitlin, "The impact of antenna diversity on the capacity of wireless communication systems," *IEEE Trans. Commun.*, vol. 42, no. 2/3/4, pp. 1740–1751, February/March/April 1994.

[3] Sergio Verdú, "Minimum probability of error for asynchronous Gaussian multiple-access channels," *IEEE Trans. Inform. Theory*, vol. IT-32, no. 1, pp. 85–96, Jan. 1986.

[4] Mahesh K. Varanasi and B. Aazhang, "Multistage detection in asynchronous code division multiple-access communications," *IEEE Trans. Commun.*, vol. COM-38, no. 4, pp. 509–519, Apr. 1990.

[5] A. J. Viterbi, "Very low rate convolutional codes for maximum theoretical performance of spread spectrum multiple access channels," *IEEE J. Select. Areas Commun.*, vol. 8, no. 4, pp. 641–649, May 1990.

[6] Jack Holtzman, "DS/CDMA successive interference cancellation," in *Proc. of ISSSTA'94*, Oulu, Finland, July 1994, pp. 69–78.

[7] Zhenhua Xie, Robert T. Short, and Craig K. Rushforth, "A family of suboptimum detectors for coherent multiuser communications," *IEEE J. Select. Areas Commun.*, vol. 8, no. 4, pp. 683–690, May 1990.

[8] Alexandra Duel-Hallen, "Equalizers for multiple input/multiple output channels and PAM systems with cyclostationary input sequences," *IEEE J. Select. Areas Commun.*, vol. 10, no. 3, pp. 630–639, Apr. 1992.

[9] Brent R. Petersen and David D. Falconer, "Suppression of adjacent-channel, cochannel and intersymbol interference by equalizers and linear combiners," *IEEE Trans. Commun.*, vol. 42, no. 12, pp. 3109–3118, Dec. 1994.

[10] David D. Falconer, Majeed Abdulrahman, Norm W. K. Lo, Brent R. Petersen, and Asrar U. H. Sheikh, "Advances in equalization and diversity for portable wireless systems," *Digital Signal Processing: A Review Journal*, vol. 3, no. 3, pp. 148–162, July 1993.

[11] Ramon Schlagenhaufer, Abu B. Sesay, and Brent R. Petersen, "A wireless multiuser system using diversity," in *Conf. Rec. IEEE VTC 99*, Houston, Texas, May 1999, pp. 2024–2028.

[12] Martin V. Clark, Larry J. Greenstein, William K. Kennedy, and Mansoor Shafi, "Optimum linear diversity receivers for mobile communications," *IEEE Trans. Veh. Technol.*, vol. 43, no. 1, pp. 47–56, Feb. 1994.

[13] Philip Balaban and Jack Salz, "Dual diversity combining and equalization in digital cellular mobile radio," *IEEE Trans. Veh. Technol.*, vol. 40, no. 2, pp. 342–354, May 1991.

[14] Srikanth Subramanian, *A Multiple-Antenna-Multiple-Equalizer System for CDMA Indoor Wireless Systems*, Ph.D. thesis, University of Victoria, B.C., Canada, 1997.

[15] Abdelgader M. Legnain, David D. Falconer, and Asrar U. H. Sheikh, "Centralized decision feedback adaptive combined space-time detector for CDMA systems," in *Conf. Rec. IEEE VTC 99*, Vancouver, BC, Canada, June 1999, vol. 2, pp. 932–936.

[16] John G. Proakis, *Digital Communications*, McGraw-Hill, New York, NY, third edition, 1995.

[17] G. J. Foschini and J. Salz, "Digital communications over fading radio channels," *The Bell System Techn. J.*, vol. 62, no. 2, pp. 429–456, Feb. 1983.

[18] Burton R. Saltzberg, "Intersymbol interference error bounds with application to ideal bandlimited signaling," *IEEE Trans. Inform. Theory*, vol. IT-14, no. 4, pp. 563–568, July 1968.

[19] Pedro M. Crespo, Michael L. Honig, and Jawad A. Salehi, "Spread-time code-division multiple access," *IEEE Trans. Commun.*, vol. 43, no. 6, pp. 2139–2148, June 1995.

[20] A. Roger Kaye and Donald A. George, "Transmission of multiplexed PAM signals over multiple channel and diversity systems," *IEEE Trans. Commun. Techn.*, vol. 18, no. 5, pp. 520–526, Oct. 1970.

[21] W. van Etten, "An optimum linear receiver for multiple channel digital transmission systems," *IEEE Trans. Commun.*, vol. 23, no. 8, pp. 828–834, Aug. 1975.

[22] L. Vandendorpe, J. Louveaux, B. Maison, and A. Chevreuil, "About the asymptotic performance of MMSE MIMO DFE for filter-bank based multicarrier transmission," *IEEE Trans. Commun.*, vol. 47, no. 10, pp. 1472–1475, Oct. 1999.

[23] N. Wiener and P. Masani, "The prediction theory of multivariate stochastic processes: I. the regularity condition," *Acta Mathematica*, vol. 98, 9-573805, pp. 111–150, Nov. 1957.

[24] Rayhan Behin, "Multi-antenna indoor radio channel measurement and analysis," Technical report, TR*Labs*, Calgary, AB, Canada, May 1998.

[25] Peter Monsen, "MMSE equalization and interference on fading diversity channels," *IEEE Trans. Commun.*, vol. COM-32, no. 1, pp. 5–12, Jan. 1984.